Sigma J Eng Nat Sci, Vol. 42, No. 2, pp. 475–489, April, 2024

Sigma Journal of Engineering and Natural Sciences
Web page info: https://sigma.yildiz.edu.tr
DOI: 10.14744/sigma.2024.00039

Research Article

Experimental analysis of a shake table test of strip footing on two layered reinforced soil

Litan DEBNATH[1,*]

[1]*Department Civil Engineering, SR University, Warangal, Telengana, 506371,India*

ARTICLE INFO

Article history
Received: 21 April 2022
Accepted: 20 June 2022

Keywords:
Shake Table; Reinforced Soil; Layered Soil; Root Mean Square Amplification; c – ϕ Soil

ABSTRACT

This paper represents both experimental and numerical study of the strip footing resting on two layered reinforced c-ϕ soil. Small scale shake table tests are conducted to evaluate the different parameters like vertical settlement, (Root mean square amplification) RMSA factor, and total stress at different levels of layered soil. Test results revealed that increase in moisture content the parameters like vertical deformation, RMSA are increasing and after the optimum moisture content the above parameters are decreasing. Further addition of moisture content increases the above parameters. Inclusion of reinforcement tends to reduce all the above parameters but is more effective in reduction of maximum RMSA amplification factor. From the numerical result, it is seen that by increasing the moisture content vertical deformation and RMSA factor is increasing by 5-10%. To verify the results obtained from the present study, a numerical analysis is done by using PLAXIS 2D and the acceptability of model is discussed. It is observed the differences between experimental and numerical results are varying from 2-6%.

Cite this article as: Debnath L. Experimental analysis of a shake table test of strip footing on two layered reinforced soil. Sigma J Eng Nat Sci 2024;42(2):475–489.

INTRODUCTION

Failures in the earthquake induced foundations are always dangerous as a whole which causes fatal damages to structures such as residential houses, bridges, retaining walls (Chu et al. [1]; Huang [2]; Huang and Chen [3]; Hyodo et al. [4]; Koseki et al. [5]; Nakamura et al. [6]; Pradel et al. [7]; Tatsuoka et al. [8]) that result in casualities. After 1995, Hyogoken-Nambu earthquake, a research has done by Tatsuoka et al. [8]. They investigated seismic stability of retaining wall as well as embankments, shows that in all retaining structures failures, bearing capacity failure played a key role. In 1999 Taiwan chi earthquake, this matter prevailed again. Huang and Chen [3] and Huang [2] carried out the post earthquake occurred in Taiwan.

The investigation was carried out in extremely damaged soil retaining walls subjected to horizontal displacement as well as vertical displacement. The seismic response in certain soil structures have been calculated using various laboratory experiments using tilting box apparatus. These experiments have done by various researchers (Koseki et al. [9]; Huang et al. [10]), dynamic (or cyclic) centrifuge tests (Kagawa et al. [11]; Dashti et al. [12]; Enomoto and

*Corresponding author.
*E-mail address: litan.debnath@sru.edu.in

This paper was recommended for publication in revised form by Regional Editor Ahmet Selim Dalkilic

Sasaki [13]; Kokkali and Anastasopoulos [14]), large-scale shaking table tests (Ling et al. [15]; Antonellis et al. [16]) and reduced-scale shaking table tests (Koseki et al. [9]; Wartman and Bray [17]; Nova and Sitar [18]; El-Emam and Bathurst [19]; Huang et al. [20,21]; Drosos et al. [22]; Guler and Selek [23]; Taha et al. [24]; Shinoda et al. [25]; Karimi and Dashti [26]). These studies dealt with the seismic performance of various soil structures, which also includes piled foundations, soil retaining walls, reinforced soil slopes, and filled slopes. The seismic bearing capacity and settlement of footings have been found out by considering some shake table experiments. The effect of frequency and magnitude of horizontal ground acceleration was found out in a test carried out by Al-Karni and Budhu [27] which showed critical ground acceleration, which differs in 2-9 times than the predictive formulas reported by Sarma and Iossifelis [28], Richards et al. [29], and Budhu and Al-Karni [30]. The pseudo-static nature of formulas and dynamic nature of shake table tests caused a discrepancy in the obtained outcome. The difficulties arrived when shake table is used are as follows: 1) the seismic force requires a relationship between pseudo-static inertia and ground acceleration. 2) Ultimate bearing capacity with respect of settlement is required more than the load. The shake table test cannot give the ultimate footing load. The seismic correction factor also plays a key role in geotechnical design, which may be derived from pseudo-static analysis (Sarma and Iossifelis [28]; Sawada et al. [31] ; Kumar and Rao [32]; Choudhury and Subba Rao [33]; Huang and Kang [34]), upper-bound solutions (Richards et al.[29] ; Soubra [35]; Kumar and Ghosh [36]; Yamamoto [37]), methods of stress characteristics (Casablanca and Biondi [38]), or numerical analyses (Charkraborty and Kumar [39]; Cinicioglu and Erkli [40]). Among these approaches, the numerical analysis only allows inputting excitations and provides seismic displacement of foundation (Azzam [41]; Kourkoulis et al. [42]). Failure mechanism found by pseudo-static method and numerical method is consistent enough, which is confirmed by Kourkoulis et al. [42]. In present study a number of shake table tests are carried out on a rigid strip footing placed on a two layered soil and the pseudo-static formulas are validated for seismic bearing capacity.

TESTING MATERIALS AND METHODOLOGY

Shake Table

In experimental study, an uniaxial shake table is used which consists of a base plate of dimension (1m x 1m) is fitted on smooth wheels at bottom which can move in horizontal direction on two parallel rails. A slotted disk made up of mild steel is attached with another disk of same diameter (Figure 1). Crank shaft is connected to the slotted disk and end of the crank shaft is connected to the reciprocating rod. The stroke length of the rod is 150 mm which gives a peak frequency 50 Hz so that it can produce sinusoidal motion.

Figure 1. Shake table attached with Crank Shaft and slotted disc.

The amplitude of the sinusoidal motion can be changed by changing the radial position of the pinion slotted disk. The frequency of base shaking can be adjusted by electrical variant (electrical speed control of the actuator/motor).

Soils Used

Strip Footing is resting on two layered soil consisting of soil type 1, soil type 2. Soil type 1 and soil type 2 are the typical c-ϕ soil. The soil samples are placed on Perspex box area (55x 35) cm^2. These are classified as clayey sand as per IS classification. The properties of soil are tabulated in Table 1. These properties are obtained after testing of soil in laboratories. Sieve analysis test, triaxial test, direct shear test and hydrometer tests are conducted in present study. Grain size distribution curve is shown in Figure 2.

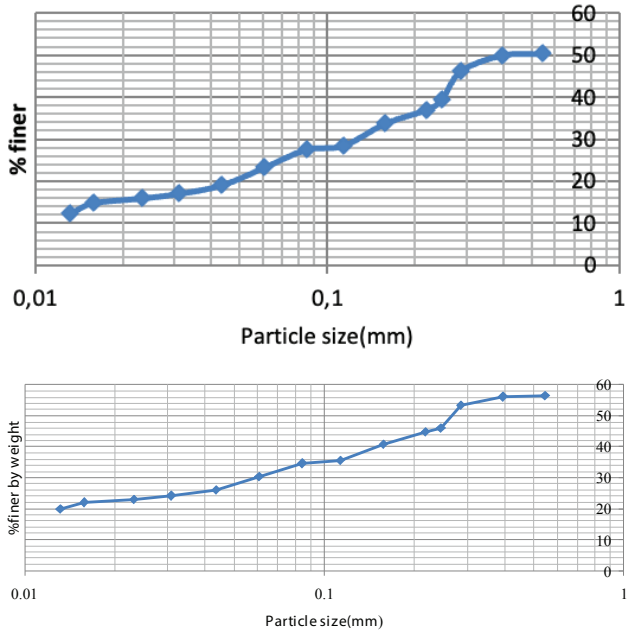

Figure 2. Grain size distribution curve for soil type 1 & type 2.

Table 1. Properties of soil 1 and soil 2

Parameter	Soil type 1	Soil type 2
Specific gravity	2.59	2.6
D_{10}, D_{30}, D_{60}	0.125,0.25,0.32	0.25,0.30,0.40
Coefficient of curvature	1.56	1.68
Coefficient of curvature	2.56	2.62
USCS classification	Silty clay	Silty clay

Reinforcement Used

Biaxial geogrids and geotextiles are used in here as reinforcement materials. Figure 3 provides the dimensional details of geogrid. The ultimate tensile strength of geogrids and geotextiles are determined as per the provisions of ASTM D 6637 and ASTM D 4595 respectively. The properties of geogrids and geotextiles tabulated in Table 2 are obtained from ASTM code is used in present analysis.

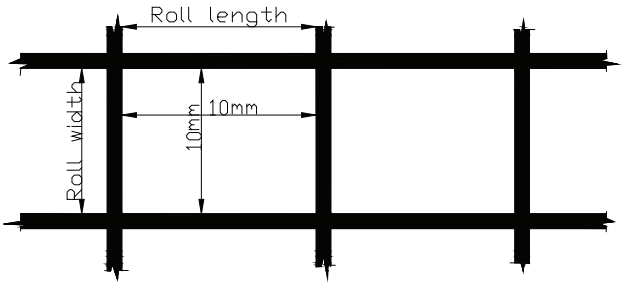

Figure 3. Dimensional details of Geogrid.

Table 2. Properties of Geogrids and geotextiles

Parameter	Geogrid	Geotextiles
Ultimate tensile strength (KN/m)	55	9.47
Yield point strain	16.60	38
Aperture size (mm)	10 x 10	NA
Aperture shape	Square	NA
Thickness (mm)	2-3	1
Secant modulus at 2% strain (KN/m^2)	219	162
Secant modulus at 5% strain (KN/m^2)	169	155.8
Mass per unit area (kg/m^2)	.22	0.21

Model Construction and Methodology

The model is constructed in a Perspex box which is 12mm thick and dimensions are 55cm×35cm×30cm (l×b×h). The sides of the Perspex box are fixed with wooden planks to prevent the horizontal movement. Schematic diagrams of typical reinforced single, two layered foundation soil are shown in Figure 4 (a) and (b). Construction process in sequence is shown in Figure 5. Each model is constructed by using 2 types of soil (soil type 1 at top, soil type 2 at bottom). Approximately 45 kg of soil is used for each model consisting of 25 kg of soil type 1, 20 kg of soil type 2. Reinforcement (geogrid/geotextile) is provided at a height of 100 mm and 180 mm from the base of the single layer, two layer reinforcement respectively as shown in Figure 4. Layered soil are tested with varying moisture content i.e. at air-dried (1%), 5%, 10%, 15% and 18%. Base accelerations are varied as 0.1g, 0.2g and 0.3g with frequencies 1 Hz, 2 Hz and 3 Hz respectively. Accelerometers (A1, A2) of type 4507 are used. A1 at the shake table and A2 on the strip which are 150 mm and 200 mm height from the bottom soil layer. These accelerometers are set in horizontal direction for measuring the vibration. The Bruel and Kjaer pulse 6.1 front end set up is used for data acquisitions.

EXPERIMENTAL RESULTS BY SHAKE TABLE TEST AND DISCUSSION

Twenty eight different shake table tests on unreinforced and reinforced layered soil models are performed in this study. These tests are performed to observe the effects of moisture content, quantity of reinforcement, various base shakings and responses at different frequencies on the stability of soils against the foundation failure. The results of the shaking table are presented in Table 3, Table 4 and Table 5. From these Tables it is observed that vertical deformation of soil increases with increasing the base shaking. It is also observed that by increasing reinforcement layer vertical deformation is decreasing

Effect of Moisture Content

Variation of maximum vertical deformation, maximum RMSA amplification factor with respect to different moisture contents (1%, 5%, 10%, 15% and 18%) for unreinforced and reinforced soil for a base shaking of 0.3g and 3 Hz frequency are measured by carrying out tests on the shake table. Figure 6(a), (b), (c) shows the variation of maximum vertical deformation (at the interface of soil 1 and soil 2) with respect to different moisture contents for the reinforced foundation soil along with the unreinforced soil. It is revealed that there is a reduction in the vertical deformation due to the increase in moisture content up to optimum moisture content of soil and thereafter there is an increase in vertical deformation due to increase in moisture content for unreinforced and reinforced foundation soil.

From Figure 7 (a-c). it is seen that RMSA amplification factor reduces gradually due to increase in moisture content. This reduction of acceleration amplification continues up to optimum moisture content of soil and thereafter acceleration amplification increases. Reinforcements on the soil reduces amplification factor up to 44% in the case of three layered geogrid reinforcement and reduces up to 34% in the case of the three layered geotextile reinforced soil. It reveals that reinforcement has significant effect on the

Table 3. Variation of vertical Displacement with water content at Base Shaking 0.3g

Type of Reinforcement	Normalized elevation	moisture content														
		1%			5%			10%			15%			18%		
		1 HZ	2 HZ	3 HZ	1 HZ	2 HZ	3 HZ	1 HZ	2 HZ	3 HZ	1 HZ	2 HZ	3 HZ	1 HZ	2 HZ	3 HZ
Unreinforced	0	2.0	2.0	2	2	2	2	2	2	2	2	2	2	2	2	2
	0.33	5.7	5.9	6	3.8	3.9	4	2.8	2.9	3	1.7	1.9	2	3.2	3.4	3.5
	0.66	8.8	8.9	9	7.7	7.9	8	6.8	6.9	7	5.8	5.9	6	6.1	6.3	6.4
	0.83	7.8	7.9	8	6.8	6.9	7	5.8	5.9	6	4.8	4.9	5	5.2	5.4	5.5
1 Layer Geotextile	0	2	2.0	2	2	2	2	2	2	2	2	2	2	2	2	2
	0.33	5.5	5.7	5.8	3.6	3.7	3.8	3.7	3.8	3.9	1.6	1.7	1.8	3.1	3.3	3.4
	0.66	8.5	8.7	8.8	7.5	7.6	7.8	6.5	6.7	6.8	5.5	5.6	5.8	6	6.1	6.2
	0.83	7.7	7.8	7.9	6.7	6.8	6.9	5.7	5.8	5.9	4.6	4.8	4.9	5.1	5.3	5.4
2 Layer Geotextile	0	2	2.0	2	2	2	2	2	2	2	2	2	2	2	2	2
	0.33	5.2	5.4	5.5	3.3	3.4	3.5	2.4	2.5	2,6	1.4	1.5	1.6	3	3.1	3.2
	0.66	8.3	8.5	8.6	7.3	7.4	7.6	6.4	6.5	6.6	5.4	5.5	5.6	5.7	5.9	6
	0.83	7.4	7.6	7.7	6.4	6.6	6.7	5.5	5.6	5.7	4.4	4.5	4.6	4.9	5.1	5.2
1 Layer Geogrid	0	2	2.0	2	2	2	2	2	2	2	2	2	2	2	2	2
	0.33	5.6	5.7	5.8	3.5	3.6	3.7	2.6	2.8	2.9	1.5	1.6	1.7	3	3.2	3.3
	0.66	8.6	8.8	8.9	7.4	7.6	7.7	6.5	6.7	6.9	5.7	5.8	5.9	5.9	6	6.1
	0.83	7.7	7.8	7.9	6.5	6.7	6.8	5.8	5.9	6	4.7	4.8	4.9	5.1	5.3	5.4
2 Layer Geogrid	0	2	2.0	2	2	2	2	2	2	2	2	2	2	2	2	2
	0.33	5.2	5.3	5.4	3.2	3.3	3.4	2.3	2.4	2.5	1.4	1.5	1.6	3	3.1	3.2
	0.66	8.2	8.4	8.5	7.2	7.4	7.5	6.5	6.6	6.7	5.4	5.5	5.6	5.7	5.8	5.9
	0.83	7.3	7.5	7.6	6.2	6.4	6.6	5.5	5.6	5.7	4.5	4.6	4.7	4.9	5.1	5.2

Table 4. Variation of RMSA Amplification with moisture content at Base Shaking 0.3g

Type of Reinforcement	Normalized elevation	Moisture content														
		1%			5%			10%			15%			18%		
		1 HZ	2 HZ	3 HZ	1 HZ	2 HZ	3 HZ	1 HZ	2 HZ	3 HZ	1 HZ	2 HZ	3 HZ	1 HZ	2 HZ	3 HZ
Unreinforced	0.00	1.00	1.00	1.00	1.00	1.00	1.00	1.00	1.00	1.00	1.00	1.00	1.00	1.00	1.00	1.0
	0.33	0.84	0.93	1.20	0.78	0.91	1.13	.73	0.81	1.04	0.72	0.77	.99	0.74	0.82	1.06
	0.66	1.35	1.51	1.94	1.27	1.46	1.82	1.17	1.31	1.68	1.16	1.24	1.59	1.19	1.33	1.71
	1.00	1.46	1.63	2.10	1.37	1.58	1.97	1.27	1.42	1.82	1.26	1.34	1.72	1.29	1.44	1.85
1 Layer Geotextile	0.00	1.00	1.00	1.00	1.00	1.00	1.00	1.00	1.00	1.00	1.00	1.00	1.00	1.00	1.00	1.00
	0.33	0.80	0.89	1.15	0.76	.85	1.09	.65	.73	0.97	.64	0.71	0.91	.69	0.77	0.99
	0.66	1.28	1.44	1.85	1.23	1.37	1.76	1.05	1.17	1.57	1.03	1.15	1.47	1.11	1.24	1.59
	1.00	1.39	1.56	2.00	1.33	1.48	1.91	1.14	1.27	1.70	1.11	1.24	1.59	1.20	1.34	1.72
2 Layer Geotextile	0.00	1.00	1.00	1.00	1.00	1.00	1.00	1.00	1.00	1.00	1.00	1.00	1.00	1.00	1.00	1.00
	0.33	0.62	0.70	0.90	0.61	.68	0.87	.56	.63	0.81	.54	0.61	0.78	.60	0.67	0.86
	0.66	1.01	1.13	1.45	0.98	1.09	1.40	0.91	1.02	1.31	.88	.98	1.27	.96	1.08	1.39
	1.00	1.09	1.22	1.57	1.06	1.18	1.52	.99	1.10	1.42	.95	1.06	1.37	1.04	1.17	1.50
1 layer Geogrid	0.00	1.00	1.00	1.00	1.00	1.00	1.00	1.00	1.00	1.00	1.00	1.00	1.00	1.00	1.00	1.00
	0.33	0.78	0.88	1.13	0.76	.85	1.09	.69	0.77	.99	.66	.73	.95	.68	0.76	0.97
	0.66	1.27	1.41	1.82	1.22	1.37	1.76	1.11	1.24	1.59	1.06	1.18	1.52	1.09	1.22	1.57
	1.00	1.37	1.53	1.97	1.32	1.48	1.90	1.20	1.34	1.72	1.15	1.28	1.65	1.18	1.32	1.70
2 Layer Geogrid	0.00	1.00	1.00	1.00	1.00	1.00	1.00	1.00	1.00	1.00	1.00	1.00	1.00	1.00	1.00	1.00
	0.33	0.60	0.67	0.86	0.56	.62	0.81	.54	0.61	0.78	.49	.54	0.70	.56	0.80	0.80
	0.66	0.96	1.08	1.39	0.90	1.01	1.30	.88	.98	1.26	.79	.88	1.14	.90	1.29	1.29
	1.00	1.04	1.17	1.50	0.97	1.09	1.41	.95	1.06	1.36	.86	.95	1.23	.97	1.40	1.40

Table 5. Variation of vertical Deformation with moisture content at Base Shaking 0.2g

Type of Reinforcement	Water content														
	1%			5%			10%			15%			18%		
	1 Hz	2 Hz	3 Hz	1 Hz	2 Hz	3 Hz	1 Hz	2 Hz	3 Hz	1 Hz	2 Hz	3 Hz	1 Hz	2 Hz	3 Hz
Unreinforced	6.70	6.90	7.00	5.30	5.40	5.60	4.60	4.80	4.90	3.60	3.70	3.90	4.80	4.9	5.0
1 Layer Geotextile	6.50	6.70	6.80	5.20	5.30	5.50	4.50	4.60	4.70	3.40	3.60	3.80	4.60	4.80	4.9
2 Layer Geotextile	6.40	6.60	6.70	5.00	5.20	5.30	4.20	4.40	4.60	3.30	3.50	3.70	4.50	4.70	4.8
1 layer Geogrid	6.40	6.60	6.80	5.00	5.30	5.40	4.20	4.40	4.60	3.40	3.50	3.80	4.60	4.80	4.90
2 Layer Geogrid	6.20	6.40	6.60	5.00	5.20	5.30	4.10	4.30	4.40	3.20	3.50	3.60	4.40	4.60	4.70

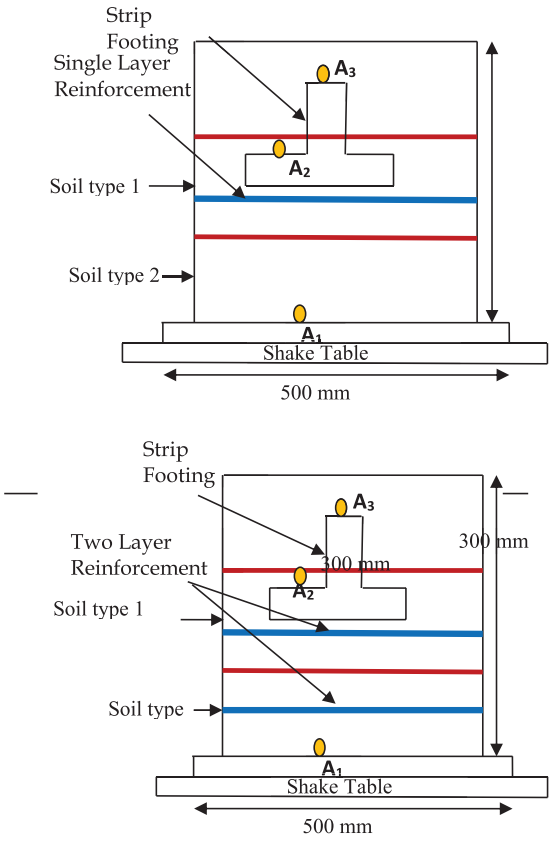

Figure 4. Schematic diagram of reinforced model test strip Footing. (a) Slope with single layer reinforcement. (b) Slope with two layer reinforcement (c) A1, A2 , A3: Accelerometers.

Figure 5. Construction process of model foundation (a) Shake Table set up (b) accelerometer connected at top and bottom of shake table.

acceleration amplification on the foundation soil but type of reinforcement has very little effect.

Effect of Quantity of Reinforcement

The test is performed by varying the quantity of reinforcement, with single layer, two layers and three layers of geogrids and geotextiles reinforcements at a base shaking of 0.3g and 3 Hz frequency. From Figure 8 (a-c) it is seen maximum vertical deformation (at the interface of soil 1 and soil 2) decreases with the increase in reinforcement quantity.

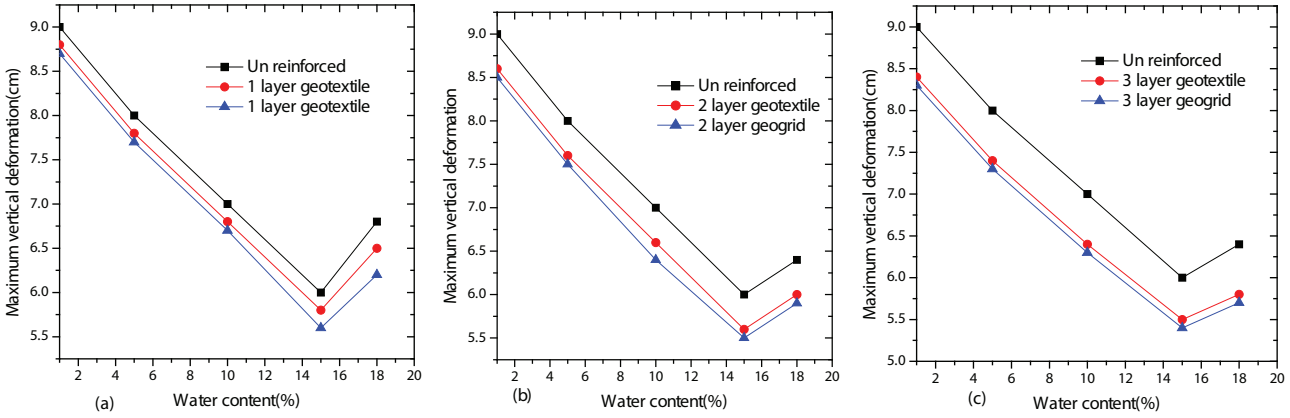

Figure 6. Effect of vertical deformation at moisture content. (a) Single layer reinforcement. (b) Two layer reinforcement. (c) Three layer reinforcement

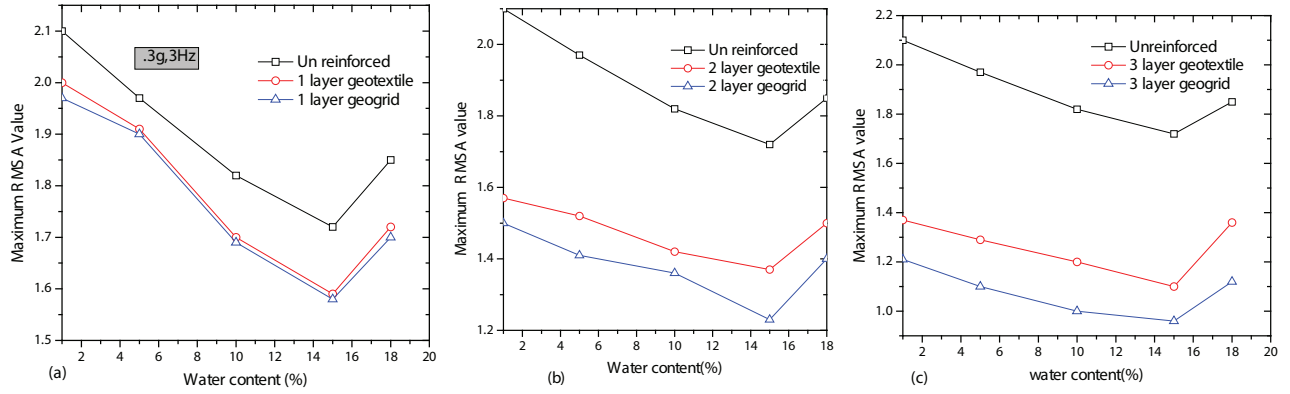

Figure 7. Effect of Root mean square amplification (RMSA) value at different water content. a) Single layer reinforcement. b) Two layer reinforcement. c) Three layer reinforcement.

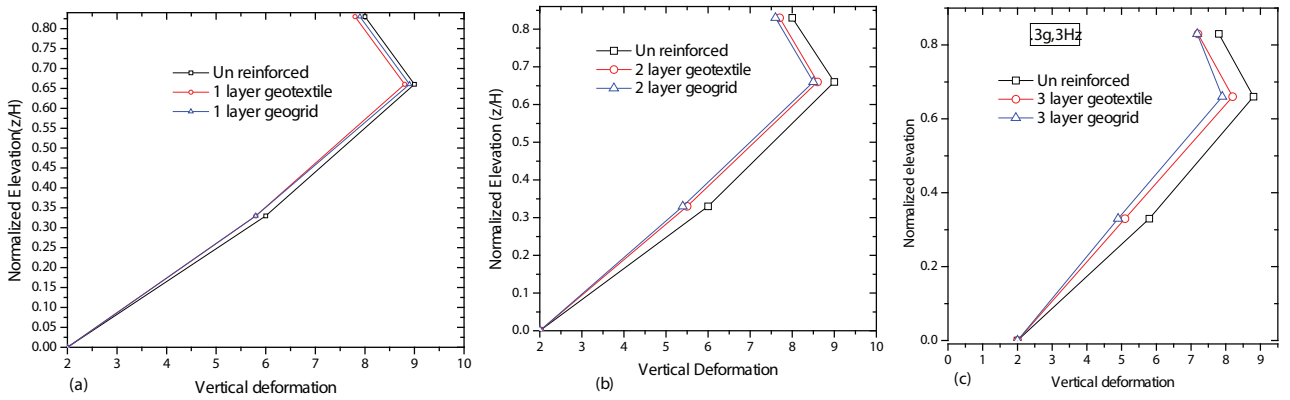

Figure 8. Effect of quantity of reinforcement on vertical deformation. (a) One layer reinforcement. (b) Two layer reinforcement. (c) Three layer reinforcement.

From Figure 9 (a-c) it is seen that acceleration amplification is greatly reduced on quantity of reinforcement. Reduction of RMSA amplification is observed in the range of 10-34% for two layered geotextile reinforced soil and 42% for two layered geogrid reinforced soil. Figure 10(a), (b) shows the acceleration response (acceleration-time) curve at top layer of the soil at air dried (w=1%) condition for base shaking 0.3g, 3Hz

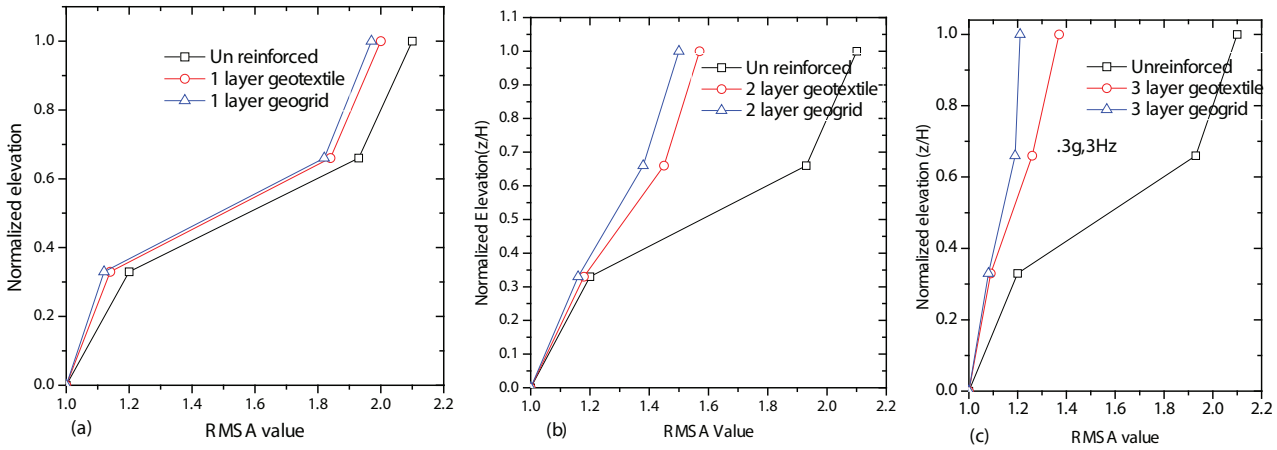

Figure 9. Effect of quantity of reinforcement on RMSA value (Root mean square amplification). (a) One layer reinforcement. (b) Two layer reinforcement. (c) Three layer reinforcement.

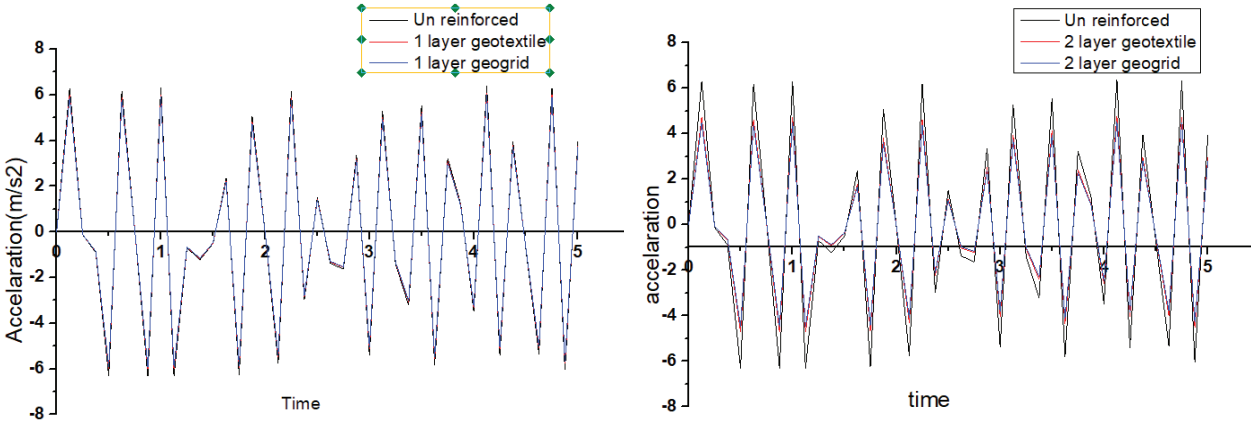

Figure 10. Acceleration response at top layer of the layered soil at base shaking 0.3g, 3Hz at air dried condition. (a) 1 layer reinforcement. (b) 2 layer reinforcement.

EFFECT OF DIFFERENT BASE SHAKING

Figures 11(a-c) represents the variation of normalized elevation with RMSA amplification at different base shaking accelerations 0.1g, 0.2g, 0.3g for a particular frequency of 3 Hz for unreinforced, 3 layered geogrid and 3 layered geotextile reinforced soil. It shows that RMSA amplification increases with the increase of base shaking acceleration. Maximum RMSA amplifications are considerably less for the reinforced foundation soil as compared to the unreinforced foundation soil.

Response of the Foundation Model at Different Frequencies

In this section a study has been carried out in order to observe the effect of different parameters like vertical deformation, RMSA factors on the reinforced soil subjected to varying frequencies of 1 Hz, 2Hz and 3Hz at a base shaking of 0.3g. From Figure 12(a-c) it is seen that vertical deformation increases with the increase of frequency. It is also seen that provision of reinforcement has an effect on the deformation of soil at different frequency level. Figure 13 (a-c) shows the variation of normalized height with respect to RMSA amplification factor of foundation model. It is observed that at a low frequency of 1Hz, the reinforced soil amplified up to 0.33 at normal height and amplified further up to a maximum value of 1. But unreinforced soil does not show the same behavior. RMSA amplification increases with the increase in normal height. In case of 2 Hz and 3 Hz frequencies, the RMSA amplification increases with the increase of normalized height.

Observed Failure Mechanism

Figure 14 (a-c) shows the typical failure mechanisms observed around the moment of failure for fixed footing with q= 55, 48 and 40 kPa, respectively under an input wave frequency 3Hz. It can be seen that failure mechanism consist a nonlinear curve shape, where a little-bit

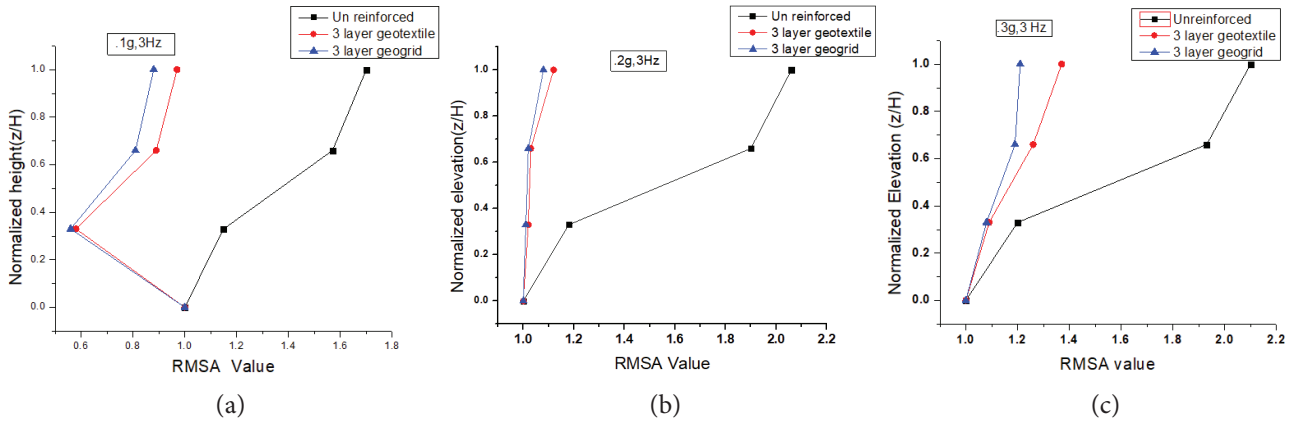

Figure 11. Variation of normalized elevation with RMSA factor for different base shaking acceleration. (a) 0.1g base shaking. (b) 0.2g base shaking. (c)0.3g base shaking.

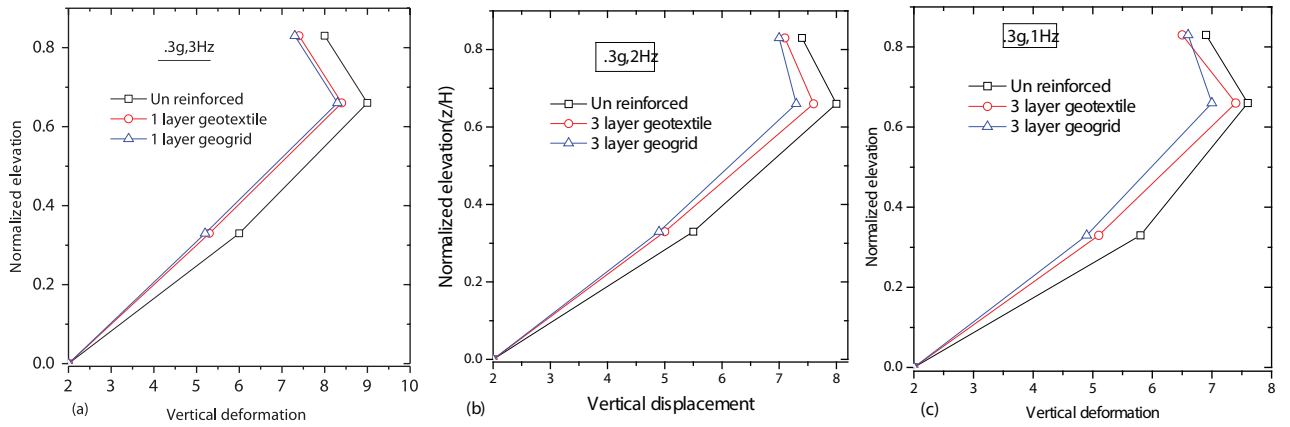

Figure 12. Variation of normalized elevation with vertical deformation at different frequency. (a) 1 Hz frequency. (b) 2 Hz frequency. (c) 3 Hz frequency.

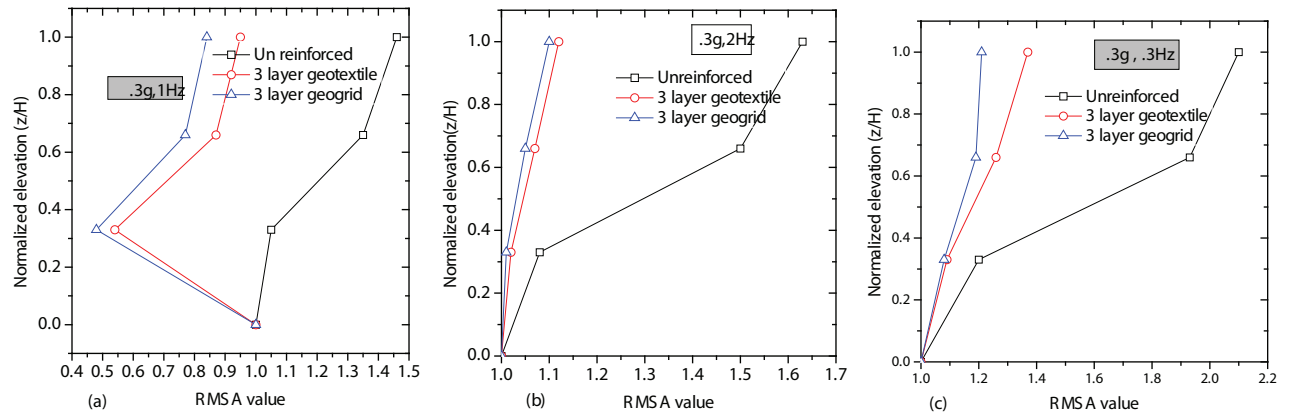

Figure 13. Variation of normalized elevation with RMSA value at different frequency. (a)1 Hz frequency. (b) 2 Hz frequency. (c) 3 Hz frequency.

of bulging occurs besides the footing. Tested are done for 0.3g with 1Hz, 2Hz and 3 Hz frequencies. A catastrophic settlement is observed for 3Hz frequency with non linear failure slip line.

(a) (b)

(c)

Figure 14. Failure mechanism observed immediately after the footing subjected 0.3g base shaking and 3Hz frequency.

NUMERICAL MODELING

To perform numerical analysis a 2D model was created and analyzed in plaxis 2D software. Matsui and San [43] considered the strength reduction technique in finite element analysis. Duncun [44] considered elastic stress strain relationship to evaluate the dependence of behavior of soil on shear strength parameters. Ugai and Leshchinsky [45] performed a comparison between 3 dimensional limit equilibrium method and finite element method. Griffiths and Lane described different finite element methods and compared them against each other. In this section, finite element analysis has been done in Plaxis2D in order to study the effect of different parameters of 2 layered soils as experimented.

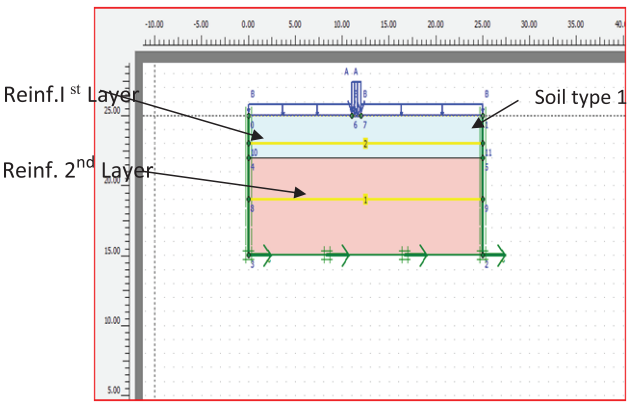

Figure 15. Geometry of the Numerical modelling (PLAXIS 2D).

Geometry of Finite Element Model Foundation

Figure 15 shows the geometric model developed in the Plaxis 2D. A full fixity boundary condition is considered and the earthquake boundary condition is generated at the base. The boundary of the model foundation soil is extended more than the actual size of the model foundation soil in both directions. The extension of the soil mass was taken 50m wide and 30 m deep. The plain strain model is used to simulate the foundation soil. The soil mass within the boundaries is divided into a number of 6 nodded triangular elements by the Plaxis mesh generator. Each node has two degree of freedom such as displacement horizontal (u) and vertical (v) directions. Small size mesh is developed by global refinement of cluster to get reliable results. The effect of ground water table is not considered in this analysis.

Loading

Standard earthquake boundaries i.e., a full fixity is applied at the base of geometry and rollers are considered at the two vertical sides of model foundation. In this study, gravitational load as well as the dynamic behavior of foundation has been generated by applying cyclic loading with amplitude and frequency for 10 s to simulate the vibration at the base as per the experimental test done on the shaking table. Only 0.3g base shaking conditions are validated for unreinforced, two layered geogrid and two layered geotextile reinforced soils.

Material Properties

After the input of boundary conditions, the material properties of the soil are entered. The Mohr coulomb failure criterions are used for modeling the foundation on two layered soils. Table 1 represents the soil properties and Table 2 represents the properties of geogrids and geotextiles reinforcements which are used for modeling in numerical analysis.

Generation of Mesh

The foundation model into divided into a number of 6 nodded triangular elements and each node has three degree freedom i) horizontal ii) vertical and iii) rotational.

NUMERICAL RESULTS, DISCUSSION AND COMPARISON OF THE RESULTS

Figures 16, 17, 18 and 19 show the deformed mesh of unreinforced and two layered geogrid reinforced layered soil due to dynamic loading at air dried (1%), 0.3g base acceleration with 3 HZ frequency. It is revealed that pattern of deformation of the reinforced layered soil is lesser than the Unreinforced layered soil for all cases.

Figures 20 and 21 shows the acceleration-time response at top and bottom layered soil for both unreinforced and reinforced soil at air dried (1%) and 5% moisture content respectively, at constant base shaking frequency of 3 Hz. It reveals that unreinforced soil accelerates more than the reinforced soil. It also reveals that as the moisture content of the soil increases from air dried (1%) to 3%, acceleration at top of the soil reduces.

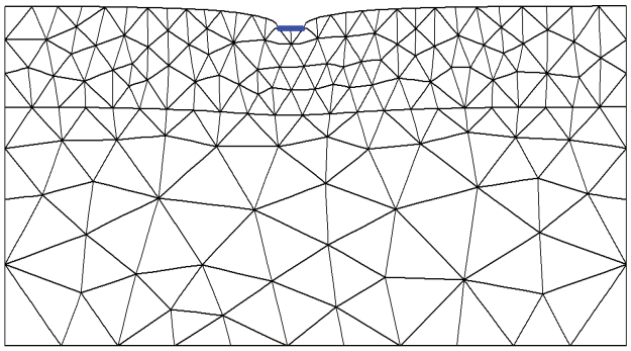

Figure 16. Unreinforced deformed mesh (0.2g, 2 Hz), extreme displacement 3.47 mm.

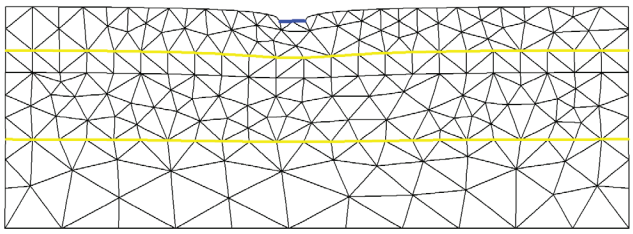

Figure 17. Reinforced deformed mesh (0.2g, 2 Hz), extreme displacement 3.42 mm.

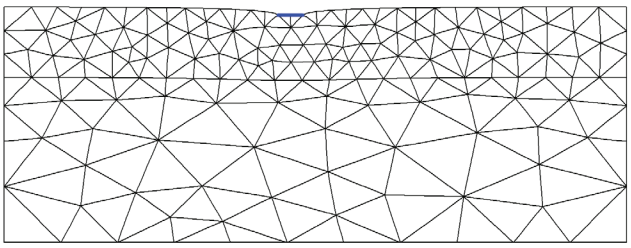

Figure 18. Unreinforced deformed mesh (0.2g, 3 Hz), extreme displacement (4.50mm)

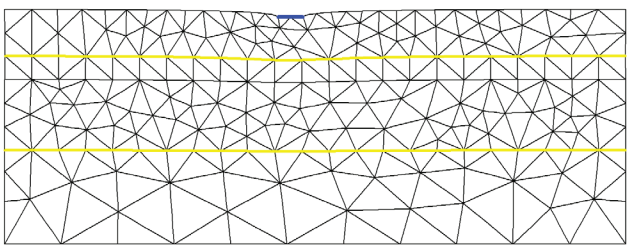

Figure 19. Reinforced deformed mesh (0.2g, 3 Hz), extreme displacement (4.43 mm).

Figures 22 and 23 shows the acceleration responses at top of the model (i.e.; top of the layered soil) due to frequency variation of 1 Hz and 3 Hz for both unreinforced and reinforced soil at air dried (1%) condition of the

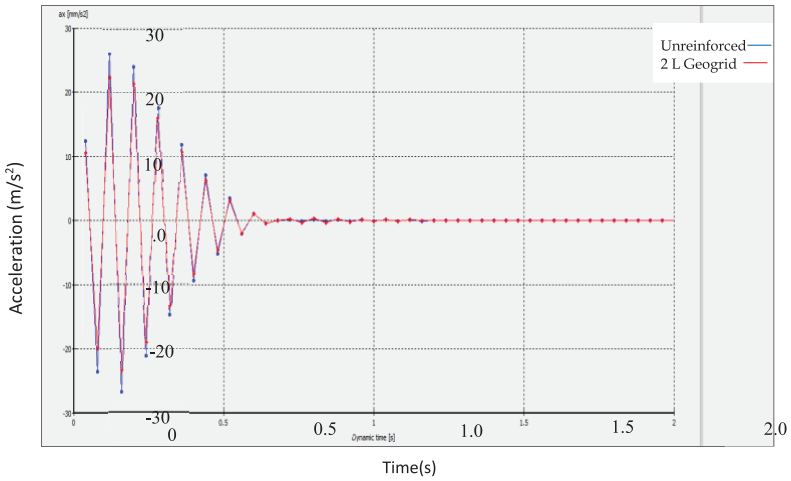

Figure 20. Acceleration response at top layer at base shaking frequency 3 Hz, air-dried(1%) condition.

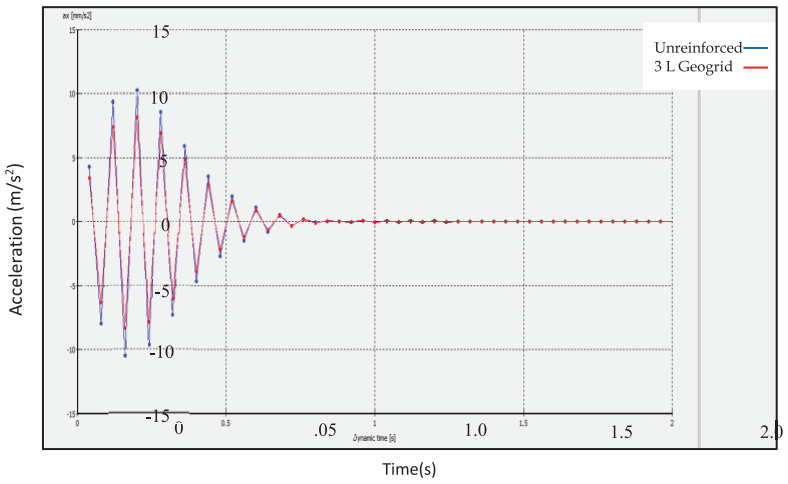

Figure 21. Acceleration response at top layer at base shaking frequency 3 Hz, water content (5%).

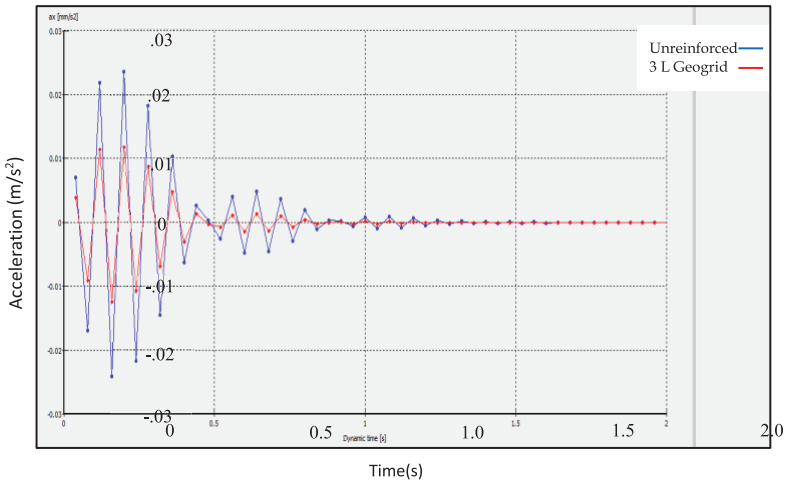

Figure 22. acceleration response at top layer at base shaking frequency 1 Hz, air-dried condition

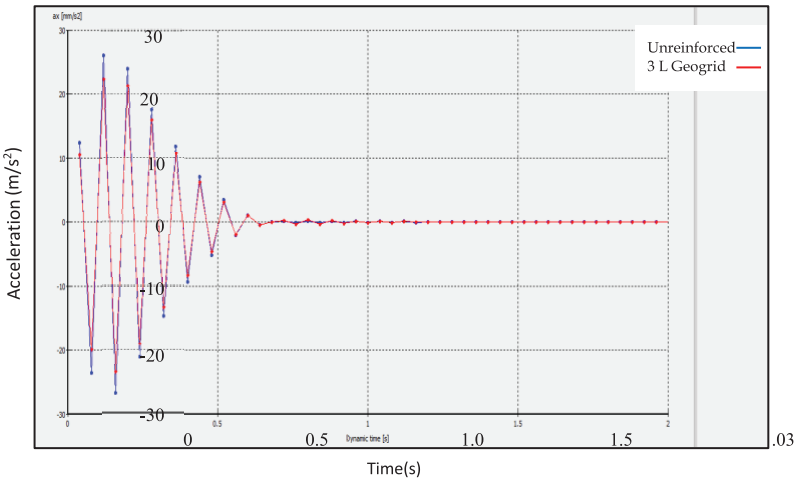

Figure 23. Acceleration response at top layer at base shaking frequency 3 Hz, air-dried condition.

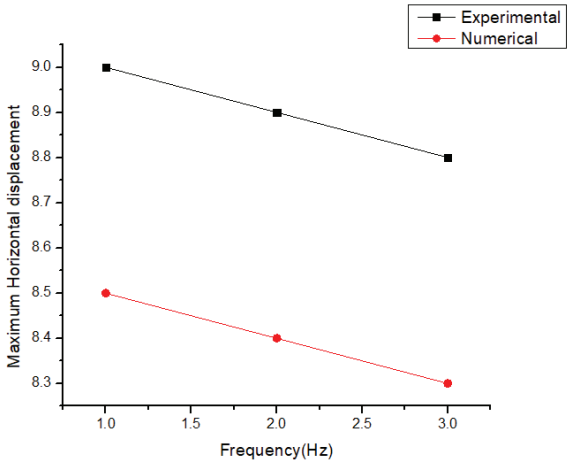

Figure 24. Comparison of experimental and numerical analysis of maximum vertical deformation for unreinforced soil.

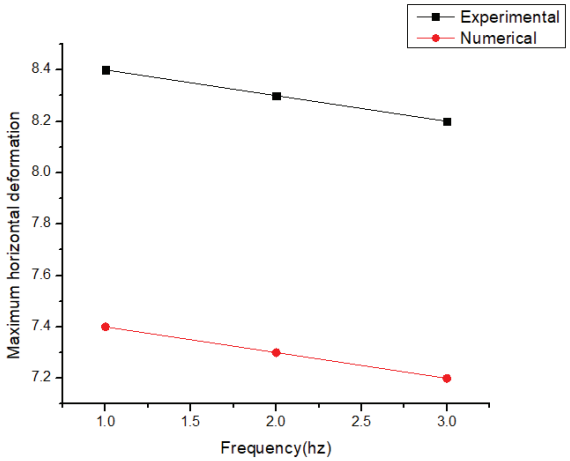

Figure 25. Comparison of experimental and numerical analysis of maximum vertical deformation for 3 layers Geogrid reinforced soil.

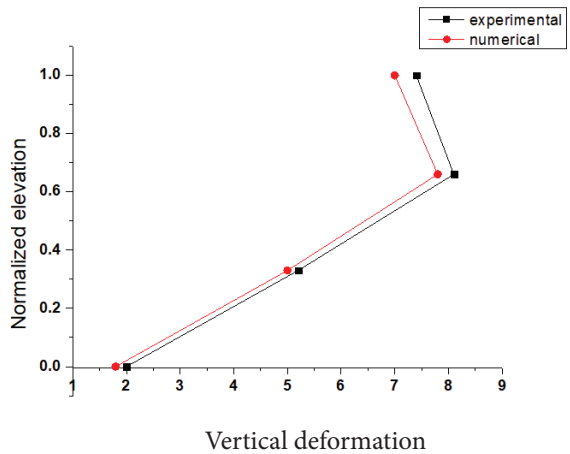

Figure 26. Comparison of experimental and numerical analysis of elevation with vertical deformation for unreinforced soil

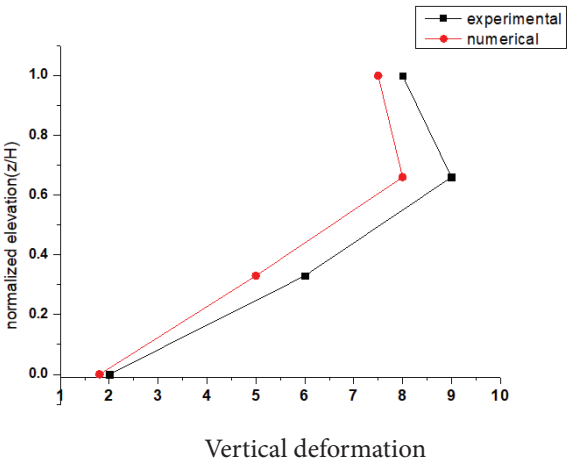

Figure 27. Comparison of experimental and numerical analysis of elevation with vertical deformation for 3 layered Geogrid reinforced soil.

foundation for a particular base acceleration of 0.3g. It is observed that comparing the figures 22 and 23, foundation model accelerates more with higher frequency shaking.

A comparison is done on the parameters of maximum vertical deformation obtained experimentally and numerically at base shaking of 0.3g at air dried condition(w=1%) with frequencies 1, 2 and 3Hz which is presented in Table 6.

Graphical comparison of the results obtained from the experiment study and numerical analysis are presented from Figures 24-27. From the comparison it is seen that both experimental and numerical results fits good.

CONCLUSION

Stability of foundation test on two layered c-ϕ soil is made under dynamic loading at varying moisture content, base shaking acceleration, frequencies, quantity and type of reinforcement. Numerical validation is done with Plaxis 2D. The following conclusions are pointed out from the present study.

- Foundation stability parameters of layered soil i.e. Maximum vertical deformation, maximum RMSA amplification factor go on decreasing as the moisture content is increased till minimum value is reached at the optimum moisture content, after which further addition of moisture content increases the above parameters.
- Inclusion of reinforcement in layered soil is very effective for reducing the parameters affecting the soil stability like maximum vertical deformation, maximum amplification factor, for all base accelerations and frequencies.
- Presence of Reinforcement in layered soil is more effective in reducing maximum RMSA amplification factor and vertical deformation.
- Geogrid reinforcement is slightly better than geotextile reinforcement for reducing parameters.
- Results obtained from the experimental studies are compared with the results obtained from numerical analysis and they have good agreement with each other.
- Further studies can be done from present investigation for multi layered soil whereas weak and strong soil layers are overlapping to each others at different height with respect to depth of foundation.

AUTHORSHIP CONTRIBUTIONS

Authors equally contributed to this work.

DATA AVAILABILITY STATEMENT

The authors confirm that the data that supports the findings of this study are available within the article. Raw data that support the finding of this study are available from the corresponding author, upon reasonable request.

CONFLICT OF INTEREST

The author declared no potential conflicts of interest with respect to the research, authorship, and/or publication of this article.

ETHICS

There are no ethical issues with the publication of this manuscript.

REFERENCES

[1] Chu DB, Stewart JP, Boulanger RW, Lin PS. Cyclic softening of low-plasticity clay and its effect on seismic foundation performance. J Geotech Geoenviron Eng 2008;134:1595. [CrossRef]

[2] Huang CC. Seismic displacement of soil retaining walls situated on slope. J Geotech Geoenviron Eng 2005;131:1108. [CrossRef]

[3] Huang CC, Chen YH. Seismic displacement of soil retaining walls situated on slope. J Geotech Geoenviron Eng 2004;130:45. [CrossRef]

[4] Hyodo M, Noda SO, Furukawa S, Furui T. Slope failures in residential land on valley fills in Yamamoto town. Soils Found 2012;52:975–986. [CrossRef]

[5] Koseki J, Koda M, Masuo S, Takasaki H, Fujiwara T. Damage to railway earth structures and foundations caused by the 2011 off the Pacific Coast of Tohoku Earthquake. Soils Found 2012;52:872–889. [CrossRef]

[6] Nakamura S, Wakai A, Umemura J, Sugimoto H, Takeshi T. Earthquake-induced landslides: Distribution, motion, and mechanism. Soils Found 2014;54:544–559. [CrossRef]

[7] Pradel D, Smith PM, Stewart JP, Raad G. Case history of landslide movement during the Northridge Earthquake. J Geotech Geoenviron Eng 2005;131:1360. [CrossRef]

[8] Tatsuoka F, Koseki J, Tateyama M, Munaf Y, Hori K. Seismic stability against high seismic loads of geosynthetic-reinforced soil retaining structures. Proc 6th Int Conf Geosynthetics, Atlanta, GA. 1998:103–142.

[9] Koseki J, Munaf Y, Tatsuoka F, Tateyama M, Kojima K. Shaking table and tilting tests of geosynthetic-reinforced soil retaining wall and conventional-type retaining wall models. Geosynth Int. 1998;5:73–96. [CrossRef]

[10] Huang CC, Horng JC, Charng JJ. Seismic stability of reinforced slopes: Effects of reinforcement properties and facing rigidity. Geosynth Int 2008;15:107. [CrossRef]

[11] Kagawa T, Minowa C, Abe A, Tazoh T. Centrifuge simulations of large-scale shaking table tests: Case studies. J Geotech Geoenviron Eng. 2004;130:663–672. [CrossRef]

[12] Dashti M, Bray JD, Pestana JM, Riemer M, Wilson D. Mechanisms of seismically induced settlement of buildings with shallow foundations on liquefiable soil. J Geotech Geoenviron Eng 2010;136. [CrossRef]
[13] Enomoto T, Sasaki T. Several factors affecting seismic behaviour of embankments in dynamic centrifuge model tests. Soils Found. 2015;55:813–828. [CrossRef]
[14] Kokkali P, Abdoun T, Anastasopoulos I. Centrifuge modeling of rocking foundations on improved soil. J Geotech Geoenviron Eng 2015;141. [CrossRef]
[15] Ling HI, Mohri Y, Leshchinsky D, Burke C, Matsushima K, Liu H. Large-scale shaking table tests on modular-block reinforced soil retaining walls. J Geotech Geoenviron Eng 2005;131:465. [CrossRef]
[16] Antonellis G, Gavras AG, Panagiotou M, Kutter BL, Guerrini G, Sander AC, et al. Shake table test of large-scale bridge columns supported on rocking shallow foundations. J Geotech Geoenviron Eng 2015;141. [CrossRef]
[17] Wartman J, Seed RB, Bray JD. Shaking table modeling of seismically induced deformations in slopes. J Geotech Geoenviron Eng 2005;131:610. [CrossRef]
[18] Nova-Roessig L, Sitar N. Centrifuge model studies of the seismic response of reinforced soil slopes. J Geotech Geoenviron Eng 2006;132:388. [CrossRef]
[19] El-Emam MM, Bathurst RJ. Influence of reinforcement parameters on the seismic response of reduced-scale reinforced soil retaining walls. Geotext Geomembr 2007;25:33–49. [CrossRef]
[20] Huang CC, Horng JC, Chang WJ, Chiou JS, Chen CH. Dynamic behavior of reinforced walls: Horizontal acceleration response. Geosynth Int 2011;17:207. [CrossRef]
[21] Huang CC, Horng JC, Chang WJ, Chiou JS, Chen CH. Dynamic behavior of reinforced walls-Horizontal displacement response. Geotext Geomembr 2011;29:257–267. [CrossRef]
[22] Drosos VT, Georgarakos ML, Loli M, Anastasopoulos O, Zarzouras G, Gazetas G. Soil foundation-structure interaction with mobilization of bearing capacity: Experimental study on sand. J Geotech Geoenviron Eng 2012;138:1369–1386. [CrossRef]
[23] Guler E, Selek O. Reduce-scale shaking table tests on geosynthetic-reinforced soil walls with modular facing. J Geotech Geoenviron Eng 2013;140. [CrossRef]
[24] Taha A, Naggar EH, Turan A. Experimental study on the seismic behavior of geosynthetic-reinforced pile-foundation system. Geosynth Int 2015;22:183–195. [CrossRef]
[25] Shinoda M, Watanabe K, Sanagawa T, Abe K, Nakamura H, Kawai T, Nakamura S. Dynamic behavior of slope models with various slope angles. Soils Found 2015;55:127–142. [CrossRef]
[26] Karimi Z, Dashti S. Seismic performance of shallow founded structures on liquefiable ground: Validation of numerical simulations using centrifuge experiments. J Geotech Geoenviron Eng 2016;142:1–13. [CrossRef]
[27] Al-Karni AA, Budhu M. An experimental study of seismic bearing capacity of shallow footings. Proc., 4th Int. Conf. on Recent Advances in Geotechnical Earthquake Engineering and Soil Dynamics, University of Missouri-Rolla. 2001;1:1–11.
[28] Sarma SK, Iossifelis IS. Seismic bearing capacity factors of shallow strip footings. Géotechnique 1990;40:265. [CrossRef]
[29] Richards R, Elms GD, Budhu M. Seismic bearing capacity and settlements of foundations. J Geotech Eng 1993;119:662. [CrossRef]
[30] Budhu M, Al-Karni A. Seismic bearing capacity of soils. Géotechnique 1993;43:181–187. [CrossRef]
[31] Sawada T, Nomachi SG, Chen WF. Seismic bearing capacity of a mounded foundation near a downhill slope by pseudo-static analysis. Soils Found 1994;34:11–17. [CrossRef]
[32] Kumar J, Rao MVBK. Seismic bearing capacity of foundations on slopes. Géotechnique 2003;53:347–361. [CrossRef]
[33] Choudhury D, Subba Rao KS. Seismic bearing capacity of shallow strip footings embedded in slopes. Int J Geomech 2006;6:176. [CrossRef]
[34] Huang CC, Kang WW. Seismic bearing capacity of a rigid footing adjacent to a cohesionless slope. Soils Found 2008;48:641. [CrossRef]
[35] Soubra AH. Upper-bound solutions for bearing capacity of foundations. J Geotech Geoenviron Eng 1999;125:59. [CrossRef]
[36] Kumar J, Ghosh P. Seismic bearing capacity for embedded footings on sloping ground. Géotechnique 2006;56:133–140. [CrossRef]
[37] Yamamoto K. Seismic bearing capacity of shallow foundations near slopes using the upper-bound method. Int J Geotech Eng 2010;4:255–267. [CrossRef]
[38] Casablanca O, Cascone E, Biondi G. The static and seismic bearing capacity factor N for footings adjacent to slopes. Procedia Eng 2016;158:410–415. [CrossRef]
[39] Chakraborty D, Kumar J. Seismic bearing capacity of shallow embedded foundations on a sloping ground surface. Int J Geomech 2015;15:1-8. [CrossRef]
[40] Cinicioglu O, Erkli A. Seismic bearing capacity of surficial foundations on sloping cohesive ground. Soil Dyn Earthquake Eng 2018;111:53–64. [CrossRef]
[41] Azzam WR. Finite element analysis of skirted foundation adjacent to sand slope under earthquake loading. Housing Building Res Center J 2015;11:231–239. [CrossRef]
[42] Kourkoulis R, Anastasopoulos I, Gelagoti F, Gazetas G. Interaction of foundation-structure systems with

seismically precarious slopes: Numerical analysis with strain softening constitutive model. Soil Dyn Earthquake Eng 2010;30:1430–1445. [CrossRef]

[43] Matsui T, San KC. Finite element slope stability analysis by shear strength reduction technique. Soils Found 1992;32:59–70. [CrossRef]

[44] Duncan JM. State of the art: limit equilibrium and finite element analysis of slopes. J Geotech Eng 1996;122:577–596. [CrossRef]

[45] Ugai K, Leshchinsky D. Three-dimensional limit equilibrium and finite element analyses: a comparison of results. Soils Found 1995;35:1–7. [CrossRef]